RELATIVE ORBIT DYNAMICS IN NEAR-GEOSTATIONARY ORBIT

Sofya Spiridonova[(1)] **and Ralph Kahle**[(2)]
[(1)]*DLR / GSOC, Münchener Str. 20, 82234 Weßling, Germany; Tel. +49(8153)28-3492, sofya.spiridonova@dlr.de*
[(2)]*DLR / GSOC, Münchener Str. 20, 82234 Weßling, Germany; Tel. +49(8153)28-2451, ralph.kahle@dlr.de*

Abstract: *A relative motion model for a Client and a Servicer spacecraft in near geostationary orbit is developed taking into account various gravitational and non-gravitational forces. In particular, differential perturbations due to Earth's oblateness, solar radiation pressure and third-body gravitational pull are studied, quantified and modeled. The relative motion model is validated using one typical far range approach test scenario against a reference generated by numerical propagation of two absolute orbits.*

Keywords: *Relative motion, orbital perturbations, geostationary orbit, on-orbit servicing.*

1. Introduction

The relative motion of two close spacecraft in Low Earth Orbit (LEO) was characterized in [1] with a focus on the secular perturbations due to Earth's oblateness as well as the differential air drag. It has been employed at the German Space Operations Center (GSOC) in various LEO formation-flying experiments, e.g. [2]. However, for two close satellites in the geostationary ring, the differential perturbations induced by the Earth's oblateness, addressed in section 3.2., are negligible, and, obviously, no air drag modeling is required. On the other hand, some effects that might be secondary in LEO can play a significant role at GEO altitude. The present research aims at extending the available relative motion model to include the perturbations of the relative motion due to the solar radiation pressure (SRP) and the third-body gravitational pull.

The effects of SRP are particularly important for communication satellites equipped with large solar arrays. The key factor driving the differential SRP perturbations in the relative orbit is the difference in area-to-mass ratio of the two spacecraft. If the objective is to provide services to various Client spacecraft within a wide range of area-to-mass ratio, SRP perturbations become an important factor in approach trajectory design and relative orbit prediction.

The lunisolar secular, long- and medium-period gravity perturbations of the relative orbit were investigated using the formulations of Kozai from [3] for absolute orbits. The theory of Kozai delivers a disturbing function which is averaged over the satellites revolution period only. Thus, the obtained perturbations depend on the actual position of the perturbing body and therefore give insight into the medium-term behavior of the satellite formation.

The relative motion model developed in [1] utilizes the following set of relative orbital elements

(ROE)

$$\delta\boldsymbol{\alpha} = \begin{pmatrix} \delta a \\ \delta\lambda \\ \delta e_x \\ \delta e_y \\ \delta i_x \\ \delta i_y \end{pmatrix} = \begin{pmatrix} (a_s - a_c)/a_s \\ (u_s - u_c) + (\Omega_s - \Omega_c)\cos i_s \\ e_{x,s} - e_{x,c} \\ e_{y,s} - e_{y,c} \\ i_s - i_c \\ (\Omega_s - \Omega_c)\sin i_s \end{pmatrix}, \tag{1}$$

where the non-singular elements

$$\boldsymbol{\kappa} = \begin{pmatrix} a \\ u \\ e_x \\ e_y \\ i \\ \Omega \end{pmatrix} = \begin{pmatrix} a \\ \omega + M \\ e\cos\omega \\ e\sin\omega \\ i \\ \Omega \end{pmatrix} \tag{2}$$

parametrize the absolute orbit of a single satellite. Here a, e, i, Ω, ω, M are the classical Keplerian elements, and the subscripts s and c refer to the Servicer and the Client. Vectors $\delta\boldsymbol{e} = (\delta e_x, \delta e_y)^T$ and $\delta\boldsymbol{i} = (\delta i_x, \delta i_y)^T$ are called the relative eccentricity and the relative inclination vectors with magnitudes denoted by δe and δi, respectively.

Along with the parametrization Eq. 1 another set of relative elements

$$\delta\boldsymbol{\kappa} = \begin{pmatrix} \delta a \\ \delta u \\ \delta e_x \\ \delta e_y \\ \delta i \\ \delta\Omega \end{pmatrix} = \begin{pmatrix} (a_s - a_c)/a_s \\ u_s - u_c \\ e_{x,s} - e_{x,c} \\ e_{y,s} - e_{y,c} \\ i_s - i_c \\ \Omega_s - \Omega_c \end{pmatrix}, \tag{3}$$

is used in the following for auxiliary computations. The relations between $\delta\boldsymbol{\alpha}$ and $\delta\boldsymbol{\kappa}$ are straightforward

$$\begin{aligned} \delta\lambda &= \delta u + \delta\Omega\cos i \\ \delta i_x &= \delta i \\ \delta i_y &= \delta\Omega\sin i. \end{aligned} \tag{4}$$

All the absolute orbital elements that appear in the following refer to those of the Servicer satellite, therefore the subscript s is dropped whenever it does not cause confusion.

The ultimate goal of this research is a high-fidelity relative motion model, which allows to predict the relative position at epoch $t + \Delta t$ taking into account SRP as well as third-body perturbations. All calculations are based on the Servicer's absolute orbital elements, obtained e.g. through orbit determination using ground station tracking data. The calculations require information on the previous relative orbital state at epoch t. Perturbations related to the Sun and the Moon depend as well on the geocentric position of the perturbing body. The absolute elements of the Client spacecraft are not required for the relative orbit prediction, and therefore this approach can be

Table 1. Spacecraft parameters

	C_R [-]	A_R $[m^2]$	Mass [kg]
Servicer	1.0	40.0	2000
Client	1.0	40.0	1000

used in design of guidance profiles towards uncooperative targets as well as on-board a Servicer spacecraft for approach strategies with high level of autonomy.

Section 2. describes a simple typical far range approach trajectory that is used as a test scenario to validate the suggested algorithm and deals separately with the evolution of the relative eccentricity and relative inclination vectors under the effects of differential SRP and third-body gravitational perturbations. Section 3. provides details on the developed Relative Motion Model (RMM), including subsections 3.2., 3.3. and 3.4. dedicated to the modeling of the differential perturbations due to oblateness, differential SRP and third-body gravitational perturbations, respectively. Section 4. provides the results of comparison with respect to the numerical propagation of two absolute orbits using full force model.

2. Basic far range approach as a test scenario

In this section a basic far range approach with a constant relative drift is simulated and illustrated in terms of relative separations along the trajectory in the Radial-Tangential-Normal (RTN) reference frame, which is formed by the coordinate axes pointing in nadir direction, along-track in-flight direction, and the direction orthogonal to the orbital frame. In this simulation, the relative trajectory as it would be in a Keplerian two-body system is considered to be the ideal guidance approach trajectory. Therefore, any perturbations arising from unequal accelerations due to various gravitational and non-gravitational disturbing forces exerted on the Servicer and the Client spacecraft are considered as deviations from the ideal guidance trajectory. To allow an efficient approach in terms of fuel consumption and manpower involved in rendezvous operations, the expected deviations from the ideal approach trajectory must be estimated beforehand and taken into account by the relative orbit control strategy.

Table 1 provides the parameters adopted for the two hypothetical spacecraft. As the Servicer might be carrying additional fuel and/or replacement units for the Client spacecraft, it was assumed that the mass of the Servicer is the double of the Clients mass.

Lets us assume that we want to approach the Client with a constant along-track drift rate of about 280 meters per orbit starting from a far range hold point 3.5 kilometers away in anti-flight direction. As the relative dynamics in a Keplerian two-body system suggests, building-up an offset of -30.0 meters in the semi-major axis of the Servicer with respect to the Client would make it advance towards the Client at the desirable rate so that by the end of the 10th day the mean relative along-track separation from the Client is about 670 meters. For the sake of the formations's safety, non-zero offsets in eccentricity and inclination vectors can be selected so that the Servicer performs additionally a Client-centered elliptical motion in the plane perpendicular to the flight direction. In the presence of large along-track errors this so-called eccentricity/inclination vector separation prevents a collision

Table 2. ROE of the initial formation geometry

	$a\delta a$ [m]	$a\delta\lambda$ [m]	$a\delta e_x$ [m]	$a\delta e_y$ [m]	$a\delta i_x$ [m]	$a\delta i_y$ [m]
ROE	-30.0	-3500.0	0.0	400.0	0.0	-100.0

risk. In a two body system the selected initial formation geometry summarized in Tab. 2 leads in to a spiral-like approach trajectory, illustrated in terms of its projections onto the planes formed by the RTN axes in Fig. 1.

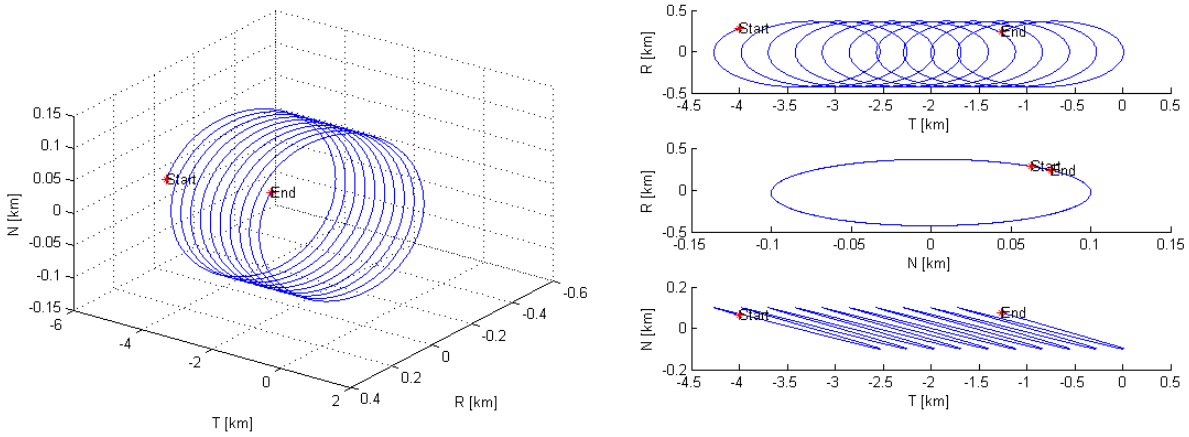

Figure 1. Ideal approach trajectory: 3D view from above (left), projections onto the RTN coordinate planes (right)

To estimate the deviations from the ideal approach trajectory that the perturbing forces might cause, a numerical propagation with a full force model – Earth gravity field of degree and order 10, SRP, Sun and Moon point mass gravitational potential – was performed for the absolute orbits of the Client and the Servicer. The resulting relative trajectory is illustrated in Fig. 2 in terms of ROE (to the left) and the projection of the relative position vector onto the planes formed by the RTN axes (to the right). The first major feature of the perturbed approach trajectory is the significant drift of the e_x component, which implies also a change in the magnitude of the relative e-vector. On the 4th day of the approach this results in zero radial separation. Provided that the along-track separation is still sufficient, this would not normally lead to a collision risk. However, the ability to predict such evolution of the relative eccentricity vector is essential for a controlled reduction of the relative separation in the plane orthogonal to the flight direction. The second major issue arises from the perturbations in the relative semi-major axis which indirectly lead to a faster along-track drift towards the Client. Thus, the Servicer overtakes the Client already on the 5th day. By the end of the 10th day, the mean along-track position of the Servicer is 1.2 kilometers away from the Client in in-flight direction. In an operational context overtaking the Client means that it is not possible to perform a v-bar approach, and the Servicer might have to perform an orbit raise maneuver to allow itself fall behind the Client again. Under the point mass gravitational force of the Earth, according to Eq. 6, the eccentricity and inclination vectors remain fixed at their initial values. Unlike that, adding solar radiation pressure to the force model for numerical propagation, introduces a long-term drift into the relative eccentricity vector. Depending on the time of the year, the drifts in the eccentricity vector are pronounces mainly in $a\delta e_x$ (around spring and autumn

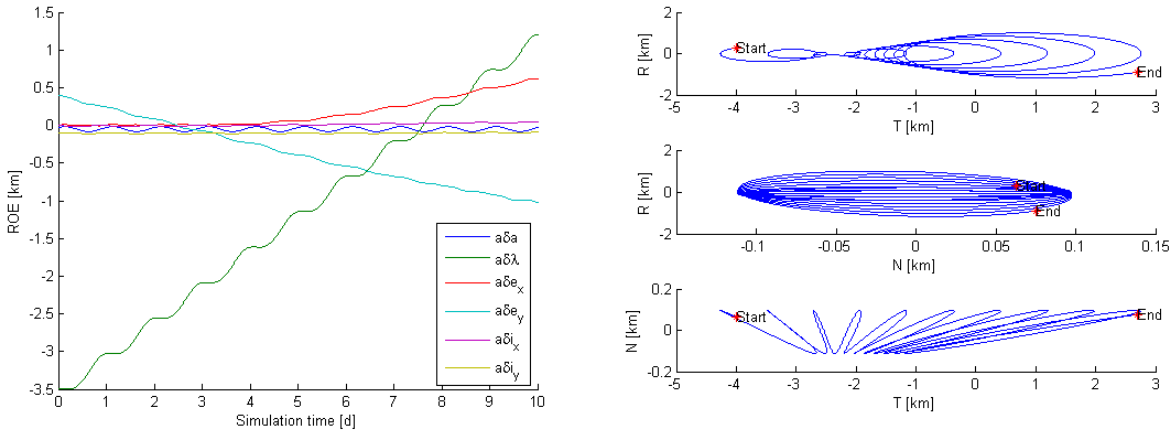

Figure 2. Perturbed approach trajectory (numerical integration of absolute orbits with full force model): ROE (left), projections onto the RTN coordinate planes (right)

equinox), or mainly in $a\delta e_y$ (around summer and winter solstice). Furthermore, SRP introduces daily perturbations into the relative inclination vector. Including the Sun and the Moon point mass gravity into the force model for numerical propagation, we observe additional long-term drifts in both vectors. The overall deviations from the ideal values at the end of the 10th days amount to 620 meters in $a\delta e_x$, 1.4 kilometers in $a\delta e_y$, 50 meters in $a\delta i_x$, and 6 meters in $a\delta i_y$, see Fig. 3.

3. Relative Motion Model

In the complete model of relative motion, the "undisturbed" ROE $a\delta\boldsymbol{\alpha}_{sphE}(t+\Delta t)$ are obtained by "propagating" the $a\delta\boldsymbol{\alpha}(t)$ according to Eq. 6, and the perturbations are calculated and added to the "undisturbed" ROE to obtain

$$\begin{aligned} a\delta\boldsymbol{\alpha}_{\text{RMM}}(t+\Delta t) = a\delta\boldsymbol{\alpha}_{sphE}(t+\Delta t) \\ + a\delta\delta\boldsymbol{\alpha}_{J_2,sec}(\boldsymbol{\kappa}, \delta\boldsymbol{\alpha}(t), \Delta t) \\ + a\delta\delta\boldsymbol{\alpha}_{J_2,sp}(\boldsymbol{\kappa}, \delta\boldsymbol{\alpha}(t), \Delta t) \\ + a\delta\delta\boldsymbol{\alpha}_{SRP}(\boldsymbol{\kappa}, \delta\boldsymbol{\alpha}(t), \boldsymbol{r}_{\text{Sun}}, \Delta t) \\ + a\delta\delta\boldsymbol{\alpha}_{Sun,sec+lp}(\boldsymbol{\kappa}, \delta\boldsymbol{\alpha}(t), \boldsymbol{r}_{\text{Sun}}, \Delta t) \\ + a\delta\delta\boldsymbol{\alpha}_{Moon,sec+lp}(\boldsymbol{\kappa}, \delta\boldsymbol{\alpha}(t), \boldsymbol{r}_{\text{Moon}}, \Delta t). \end{aligned} \tag{5}$$

As it will be discussed in the following, the perturbations with the subscript J_2 can be omitted without any noticeable loss of accuracy.

3.1. Unperturbed Relative Motion

In a Keplerian two-body system, the only relative element changing with time is the relative mean longitude $a\delta\lambda$. If the semi-major axis offset $a\delta a$ in not zero, the Servicer is drifting with respect to the Client with a rate of -$3\pi a\delta a$ per revolution. Thus, the evolution of ROE under the influence of

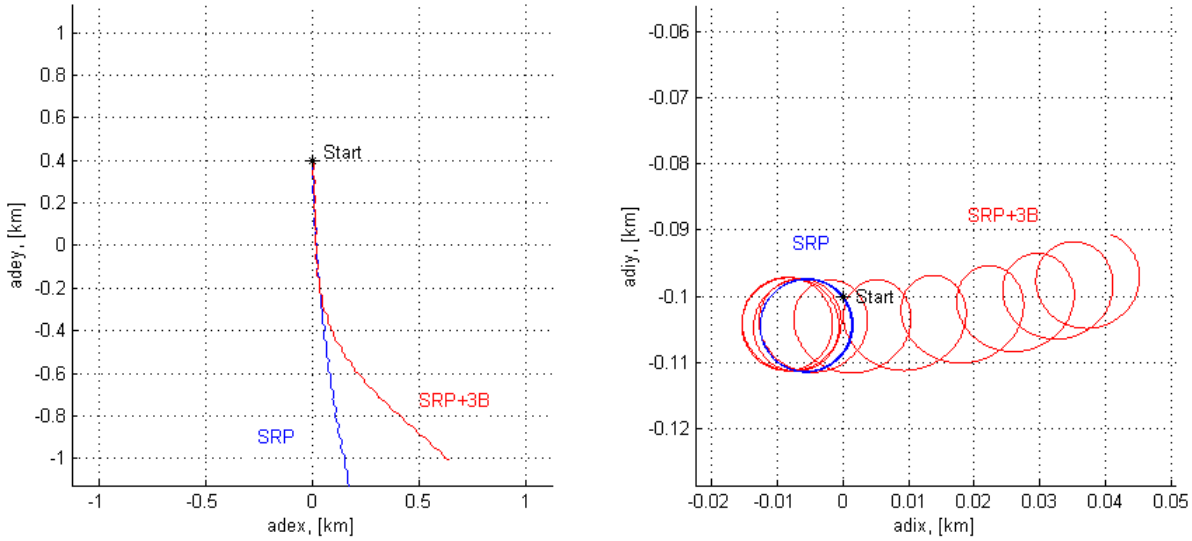

Figure 3. Evolution of the perturbed e/i vectors (numerical integration of absolute orbits): relative eccentricity vector (left), relative inclination vector (right)

the Earth's central gravity field can be formulated as

$$\delta\alpha_i(t) = \delta\alpha_{i0} - \frac{3}{2}(u(t) - u_0)\delta\alpha_{10}\delta_{i2}, \tag{6}$$

where $i = 1, \ldots, 6$ and δ_{i2} is the Kronecker delta. A more detailed analysis of the unperturbed motion can be found in [1].

Multiplied by the semi-major axis, the relative orbital elements (ROE) in Eq. 1 allow a convenient representation of the ideal relative in-plane and out-of-plane motion. Namely, in a Keplerian two-body system and under the assumption of a near-circular Servicer's orbit, and spacecraft separations which are small as compared to the orbital radius, the relative motion is bounded, if the offset in the semi-major axes $a\delta a$ is zero. In the orbital plane, the Servicer circumscribes with respect to the Client an ellipse with semi-major axis $2a\delta e$ in along-track direction and semi-minor axis $a\delta e$ in radial direction, where $a\delta e$ is the magnitude of the relative eccentricity vector. The ellipse is centered along the tangential axis at distance $a\delta\lambda$ to the Client, which is the relative mean longitude and represents mean along-track separation between the spacecraft. On the other hand, the magnitude of oscillation is the direction orthogonal to the orbital plane is equal to $a\delta i$, and the relative ellipse in RN-plane is centered on the Client.

3.2. Differential J_2 Perturbations

Secular perturbations. Secular differential perturbations due to Earths oblateness term J_2 for near-circular close orbits can be linearly approximated as

$$\delta\delta\dot{\boldsymbol{\alpha}}_{J_2,sec} = \begin{pmatrix} 0 \\ -\frac{21}{2}\gamma n \sin 2i \ \delta i_x \\ -\frac{3}{2}\gamma n \left(5\cos^2 i - 1\right) \ \delta e_y \\ \frac{3}{2}\gamma n \left(5\cos^2 i - 1\right) \ \delta e_x \\ 0 \\ 3\gamma n \sin^2 i \ \delta i_x \end{pmatrix}, \tag{7}$$

where $\gamma = \frac{J_2}{2}\left(\frac{R_E}{a}\right)^2 \frac{1}{(1-e^2)^2}$ and R_E is the Earth's equatorial radius, [1].

Examining closely the multiplication factors, we expect that the highest perturbation will be observed in the eccentricity vector, since the perturbations in $\delta\lambda$ and δi_y contain small quantities $\sin 2i$ and $\sin^2 i$. Moreover, factor γ is about 37 times lower than in LEO orbit of e.g. 500 km. Taking into account that also the mean motion n is about 15 times smaller that in LEO orbit, we can already assume that the secular perturbations due to J_2 are very small in magnitude. More precisely, considering the initial $a\delta e_x = 0$m, and $a\delta e_y = 400$m, the secular drift is $-2.2 \cdot 10^{-6}$ m/s in $a\delta e_x$ and 0 m/s in $a\delta e_y$. After 10 days the deviation in $a\delta e_x$ from the initial ideal value is merely 1.9 meters. Comparing this value with the magnitude of third-body perturbations analyzed in section 3.4., we conclude that the secular perturbation due to J_2 are by two orders of magnitude lower, and therefore can be omitted from the relative motion model.

Short-period perturbations. A short quantification analysis of the short-period perturbations can be performed based on the analytical developments for orbits of small eccentricities listed by Eckstein in [4]:

$$\begin{aligned}
\delta a &= \frac{3a}{2\lambda'} G_{20} \sin^2 i \cos 2u \quad \delta u = \frac{3}{4\lambda'} G_{20} \left(4\sin^2 i - 1\right) \sin 2u \\
\delta e_x &= \frac{3}{2\lambda'} G_{20} \left[\left(1 - \frac{5}{4}\sin^2 i\right) \cos u + \frac{7}{12}\sin^2 i \cos 3u \right] \\
\delta e_y &= \frac{3}{2\lambda'} G_{20} \left[\left(1 - \frac{7}{4}\sin^2 i\right) \sin u + \frac{7}{12}\sin^2 i \sin 3u \right] \\
\delta i &= \frac{3}{8\lambda'} G_{20} \sin 2i \cos 2u \quad \delta\Omega = \frac{3}{4\lambda'} G_{20} \cos i \sin 2u,
\end{aligned} \tag{8}$$

where

$$\lambda' = 1 + \frac{3}{2} G_{20}(3 - 4\sin^2 i), \quad G_{20} = J_2 \left(\frac{R_E}{a}\right)^2, \quad J_2 = 1.082 \cdot 10^{-3}.$$

This formulation of the perturbations in the *absolute* orbital elements of a single satellite can be

used to approximate linearly the perturbations of the *relative* orbital elements by introducing small variations of $\delta\boldsymbol{\kappa}$ and building the Jacobian matrix of the non-linear system in Eq. 8. Note that the factor G_{20} contains a term $\frac{1}{a^2}$, which makes it 36 times smaller than the corresponding factor for LEO. Again, this allows us to neglect in the relative motion model the short-period perturbations due to Earth oblateness.

3.3. Differential SRP Perturbations

To take SRP into account the simplest cannonball model can be used according to which the absolute acceleration due to SRP is

$$\delta\ddot{\boldsymbol{r}} = -P_{\odot} C_R \frac{A_R \boldsymbol{r}_{\odot}}{m \, r_{\odot}^3} \mathrm{AU}^2, \tag{9}$$

where $P_{\odot}$ is the constant of the solar radiation pressure, and $\boldsymbol{r}_{\odot}$ is the relative position vector of the spacecraft with respect to the Sun. Note that the symbol δ in front of $\ddot{\boldsymbol{r}}$ implies here that this acceleration is of perturbational character, yet absolute.

Given the large distance to the sun as compared to the distance between the satellites it suffices to assume that the distance to the sun and the unit direction-to-the-sun vector are the same for both spacecraft. In such way the differential SRP coefficient

$$\mathrm{DB}_{\mathrm{SRP}} = C_{R_s} \frac{A_{R_s}}{m_s} - C_{R_c} \frac{A_{R_c}}{m_c}$$

is the only parameter of influence, and the differential perturbational acceleration can be approximated as

$$\delta\delta\ddot{\boldsymbol{r}} = -P_{\odot} \mathrm{DB}_{\mathrm{SRP}} \frac{\boldsymbol{r}_{\odot}}{r_{\odot}^3} \mathrm{AU}^2. \tag{10}$$

The differential acceleration in Earth-centered inertial system delivered by Eq. 10 can be integrated assuming that it remains constant during the integration time Δt. Obtained perturbations in the relative velocity and position vectors can be transformed to the orbital RTN reference frame using the orbital information of the Servicer. After that the linear relations from [1] between ROE and relative Cartesian state can be used to approximate the perturbations in ROE. To conclude the description of the SRP part od the relative motion model, it should be mentioned that during the spring and autumn eclipse periods, satellites in near-geostationary orbit pass once per day through the Earth's shadow, which is included into the model through a shadow function ν as described in [5].

3.4. Differential Third-Body Perturbations

This section analyzes secular and long-period lunisolar perturbations in ROE based on linearizing the equations for the differential perturbations in terms of the variations of the absolute relative elements. For that, the Lagrange equations are used relating the rates of the non-singular absolute

elements $\boldsymbol{\kappa}$ to the partial derivatives of the disturbing potential with respect to $\boldsymbol{\kappa}$:

$$\begin{aligned}
\frac{da}{dt} &= \frac{2}{na}\frac{\partial R}{\partial u} \\
\frac{de_x}{dt} &= \frac{\eta}{na^2}\left(\frac{\partial R}{\partial e_y} + \frac{e_x}{1+\eta}\frac{\partial R}{\partial u}\right) + \frac{e_y \cot i}{na^2\eta}\frac{\partial R}{\partial i} \\
\frac{de_y}{dt} &= \frac{\eta}{na^2}\left(\frac{\partial R}{\partial e_x} - \frac{e_y}{1+\eta}\frac{\partial R}{\partial u}\right) - \frac{e_x \cot i}{na^2\eta}\frac{\partial R}{\partial i} \\
\frac{di}{dt} &= \frac{\cot i}{na^2\eta}\left(e_x\frac{\partial R}{\partial e_y} - e_y\frac{\partial R}{\partial e_x} + \frac{\partial R}{\partial u}\right) - \frac{\csc i}{na^2\eta}\frac{\partial R}{\partial \Omega} \\
\frac{d\Omega}{dt} &= \frac{\csc i}{na^2\eta}\frac{\partial R}{\partial i} \\
\frac{du}{dt} &= n - \frac{2}{na}\frac{\partial R}{\partial a} + \frac{\eta}{1+\eta}\frac{1}{na^2}\left(e_y\frac{\partial R}{\partial e_y} + e_x\frac{\partial R}{\partial e_x}\right) - \frac{\cot i}{na^2\eta}\frac{\partial R}{\partial i},
\end{aligned} \tag{11}$$

where $\eta = \sqrt{1 - e_x^2 - e_y^2}$ and R is the so-called disturbing function or perturbing potential such that $F = \dfrac{\mu}{2a} + R$, where F is the total force function, i.e

$$F = V + R - T = \frac{\mu}{r} + R - \frac{v^2}{2} = \frac{\mu}{2a} + R,$$

V and T being the undisturbed potential and the kinetic energy respectively. Taking into account that $\boldsymbol{\kappa}(i) = \boldsymbol{\kappa}_0(i) + nt\delta_{i2} + \delta\boldsymbol{\kappa}$, where $i = 1, \ldots, 6$ and δ_{i2} is the Kronecker delta which introduces a secular change in u, the same Lagrange equations are valid for the perturbations $\delta\boldsymbol{\kappa}$ with the difference that the term n disappears from the equation for $\dot{u}$.

In the following, the Lagrange equations will be used for $\delta\boldsymbol{\kappa}$. Note that here $\delta\boldsymbol{\kappa}$ refers to the perturbations in the absolute orbital elements in Eq. 2, and not to the relative orbital elements from Eq. 3.

In the following, the theory developed in [3] by Y. Kozai for single satellites in near-geostationary orbit will be applied. In [3], the disturbing function for lunar and solar gravity perturbations was expressed as a function of the Keplerian elements of the satellite and the polar coordinates of the Sun and the Moon. To obtain the secular and long-period terms, the disturbing function was averaged with respect to the mean anomaly of the satellite.

To use the disturbing function from [3] for our analysis, we need to re-write it in terms of the

non-singular elements from Eq. 2. This leads to the formulation

$$
\begin{aligned}
R = n'^2 a^2 \left(\frac{a'}{r'}\right)^3 \beta \cdot \Bigg\{ & \frac{1}{16}\Big(3\cos^2\delta(2-\sin^2 i) + 6\sin^2 i \sin^2\delta - 4 - 6\sin i \sin 2\delta \sin(\Omega-\alpha) \\
& + 3\sin^2 i \cos^2\delta \cos 2(\Omega-\alpha)\Big)\cdot\left(2+3e_x^2+3e_y^2\right) + \frac{15}{8}\Big(\cos^2\delta\left[\left(e_x^2-e_y^2\right)\cos 2(\Omega-\alpha)\right. \\
& \left. - 2e_x e_y \sin 2(\Omega-\alpha)\right] + \sin i \sin 2\delta\left[\left(e_x^2-e_y^2\right)\sin(\Omega-\alpha) + 2e_x e_y \cos(\Omega-\alpha)\right]\Big) \\
& - \frac{15}{32}\left(\frac{a}{a'}\right)\left(\frac{a'}{r'}\right)\Big(2\cos\delta\left(5\cos^2\delta-4\right)\left[e_x\cos(\Omega-\alpha) - e_y\sin(\Omega-\alpha)\right] \\
& + 4\sin i \sin\delta\left(5\cos^2\delta-2\right)e_y - 5\sin i \sin 2\delta\cos\delta\left[e_x\sin 2(\Omega-\alpha) + e_y\cos 2(\Omega-\alpha)\right]\Big) \\
& + \frac{3}{64}\left(\frac{a}{a'}\right)^2\left(\frac{a'}{r'}\right)^2\Big(35\cos^4\delta - 40\cos^2\delta + 8 - 10\sin i\sin 2\delta\left(7\cos^2\delta-4\right)\sin(\Omega-\alpha)\Big) \\
& - \frac{105}{128}\left(\frac{a}{a'}\right)^3\left(\frac{a'}{r'}\right)^3\left(21\cos^4\delta - 28\cos^2\delta + 8\right)\cos\delta\left(e_x\cos(\Omega-\alpha) - e_y\sin(\Omega-\alpha)\right)\Bigg\},
\end{aligned}
$$

where the motion of the Sun or the Moon is parametrized by the geocentric distance r', right ascension α, and declination δ. These parameters can be found from geocentric rectangular coordinates

$$
\begin{aligned}
x' &= r'\cos\delta\cos\alpha \\
y' &= r'\cos\delta\sin\alpha \\
z' &= r'\sin\delta.
\end{aligned}
$$

In the development of R, primed quantities n' and a' denote the mean motion and the semi-major axis of the perturbing body, while

$$
\beta = \begin{cases} 1 & \text{for the Sun} \\ \frac{m'}{m+m'} & \text{for the Moon} \end{cases},
$$

where m is the mass of the Earth and m' is the mass of the Moon.

Expressing the Lagrange equations for perturbations and the disturbing function R in terms of the orbital elements $\boldsymbol{\kappa}$, Eq. 11 delivers the rates of the perturbations in the absolute orbital elements as non-linear functions of $\boldsymbol{\kappa}$

$$
\delta\dot{\boldsymbol{\kappa}} = \boldsymbol{F}\left(\boldsymbol{\kappa}\right). \tag{12}
$$

Provided that $\boldsymbol{F}$ is differentiable at point $\boldsymbol{\kappa}$ and assuming that the separation between the satellites is small, we can approximate linearly the rates of the differential perturbations as

$$
\delta\delta\dot{\boldsymbol{\kappa}} = J_{\boldsymbol{F}}\cdot\delta\boldsymbol{\kappa}, \tag{13}
$$

where $J_{\boldsymbol{F}}$ is the Jacobian matrix of the system of equations in Eq. 12, i.e.

$$J_{\boldsymbol{F}} = \begin{pmatrix} \frac{\partial \delta \dot{a}}{\partial a} & \frac{\partial \delta \dot{a}}{\partial u} & \cdots & \frac{\partial \delta \dot{a}}{\partial \Omega} \\ \frac{\partial \delta \dot{u}}{\partial a} & \frac{\partial \delta \dot{u}}{\partial u} & \cdots & \frac{\partial \delta \dot{u}}{\partial \Omega} \\ \vdots & \vdots & \ddots & \vdots \\ \frac{\partial \delta \dot{\Omega}}{\partial a} & \frac{\partial \delta \dot{\Omega}}{\partial u} & \cdots & \frac{\partial \delta \dot{\Omega}}{\partial \Omega} \end{pmatrix}. \tag{14}$$

Since the disturbing function R has been averaged over the satellite's revolution period, the first line as well as the second column in $J_{\boldsymbol{F}}$ contain only zeros. Also the first column contains values by a factor of order of $\frac{1}{a}$ smaller than the values in the columns 3 to 6.

Calculating the first and the second partial derivatives of R and substituting them into Eq. 13 we can estimate the change in ROE due to lunisolar gravitational force assuming that $\boldsymbol{\kappa}$ is constant during the propagation time step.

4. Results and Conclusion

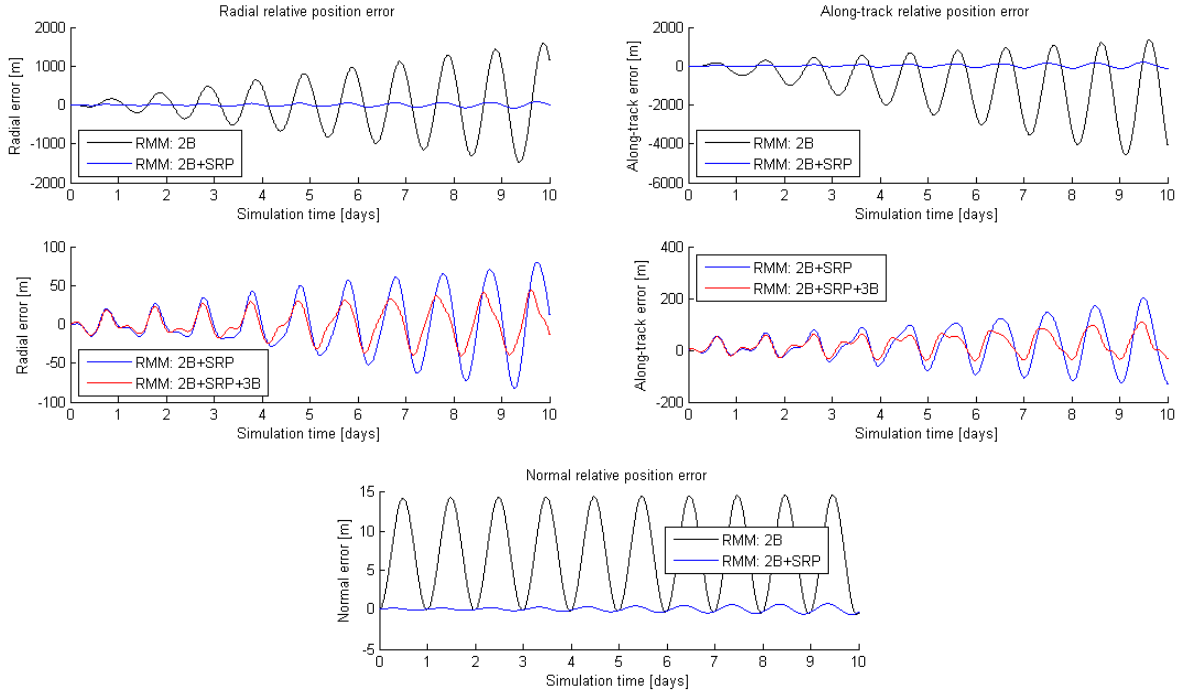

Figure 4. Propagation errors of different RMM configurations (against the numerical reference): radial (left), tangential (right), normal (bottom)

Figure 4 shows the errors of various Relative Motion Model (RMM) configurations in relative separations in radial, along-track and normal directions. Moreover, Fig. 5 illustrates in vector form

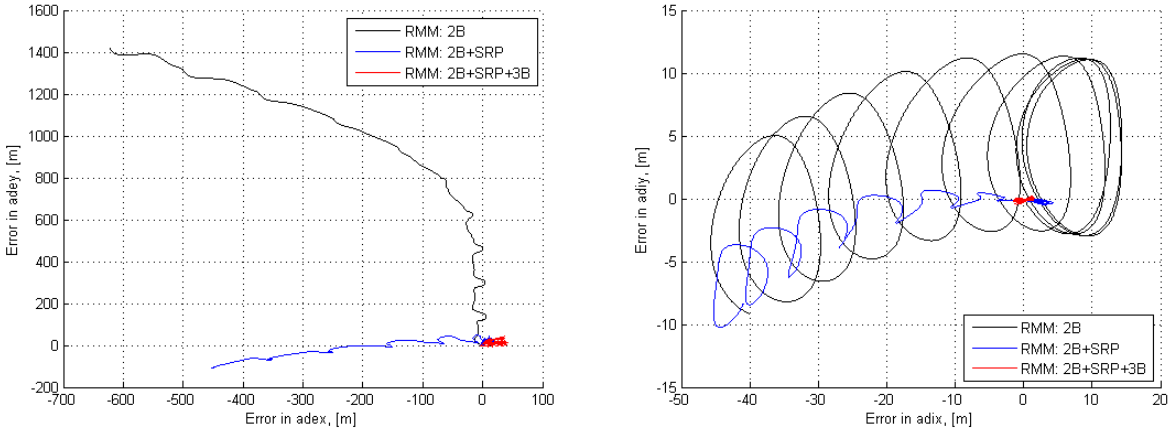

Figure 5. Propagation errors of different RMM configurations (against the numerical reference): relative eccentricity vector (left), relative inclination vector (right)

the errors of the intermediate and final RMM in estimation of the relative eccentricity and inclination vectors, respectively.

Unperturbed RMM. The amplitudes of the errors of the initial simplest RMM following Eq. 6 under the assumption of an ideal two-body Keplerian system are increasing with time both in radial and along-track directions. This is due to the growing magnitude of the difference between the ideal and the perturbed $a\delta\boldsymbol{e}$, which translates directly into the amplitude of the error oscillations in the radial direction, and with a factor of 2 is directly proportional to the amplitude of the error oscillations in the along-track direction. The errors in the tangential component show an additional growing bias due to the growing error in the mean along-track distance $a\delta\lambda$ itself (see Fig. 2 to the left). However, the amplitude of 15 meters of the oscillations in the direction orthogonal to the orbital plane, stays constant, since the magnitude of perturbed $a\delta\boldsymbol{i}$, apart from the periodic perturbations due to SRP, exhibits no secular perturbations from the third-body gravity fields. The third-body perturbations result solely in a rotation of $a\delta\boldsymbol{i}$ without changing its magnitude (see Fig. 3 to the right).

Intermediate and final RMM. Adding SRP perturbations to the relative motion model as described in section 3.3. (intermediate RMM) allows to reduce the growth of the amplitude of the error oscillations in all components and also remove the growing bias in the along-track direction. Introduction of the third-body perturbations as described in section 3.4. reduces by half the remaining errors in the radial and the along-track components. However, in the direction orthogonal to the orbital plane, due to the merely rotational effect of the third-body perturbation exerted on the relative inclination vector, there is no improvement as compared to the result of the intermediate RMM. To evaluate properly the performance of the complete RMM, we should have a look at the component-wise errors in the inclination vector. Figure 5, indeed, demonstrates the absence of any long-term error drifts in $a\delta\boldsymbol{i}$. Also the long-term error drifts in the components of $a\delta\boldsymbol{e}$ result mostly eliminated. The remaining error in the estimated $a\delta\boldsymbol{e}$ is less than 45 meters during the 10 days of the simulated approach, while the error in $a\delta\boldsymbol{i}$ stays always less than 2 meters.

Conclusions. The presented relative motion model addresses perturbations in the relative orbit due to solar radiation pressure and the gravitational potential of the Sun and the Moon. A numerical quantification analysis performed for a sample far range approach scenario demonstrates that, indeed, if not taken into account, such perturbations might pose challenges for time- and safety-critical on-orbit-servicing operations for future missions in near-geostationary orbit. A comparison with a numerically generated reference proves that the suggested model allows to eliminate long-term error drifts, as well as the most significant periodic error oscillations. The performed simulation shows that an accurate relative orbit prediction on the basis of the Servicer orbital information alone is possible up to 10 days in advance. Therefore, given sufficient computational resources, the suggested algorithm can be incorporated into automatic guidance, navigation and control algorithms on-board the Servicer spacecraft to allow fuel-efficient autonomous approaches to uncooperative targets in near-geostationary orbit.

5. References

[1] S. D'Amico, *Autonomous formation flying in low earth orbit*, Technical University of Delft, (2010).

[2] G. Gaias, S. D'Amico, J.-S. Ardaens, *Angles-only Navigation to a Non-Cooperative Satellite using Relative Orbital Elements*, Astrodynamics Specialists Conference AAS, 13-16 August 2012, Minneapolis, MN, USA.

[3] Y. Kozai, *A new method to compute lunisolar perturbations in satellite motions*, Smithsonian Astrophysical Observatory Special Report 349 (1973).

[4] M.C. Eckstein, H. Hechler, *A reliable derivation of the perturbations due to any zonal and tesseral harmonics of the geopotential for nearly-circular satellite orbits*, ESOC, ESRO SR-13 (1970).

[5] O. Montenbruck, E. Gill, *Satellite orbits: Models, Methods and Applications*, Springer Verlag, Heidelberg (2000).